Dressed-state analysis of two-color excitation schemes

Thomas K. Bracht,[1,2,*] Tim Seidelmann,[3] Yusuf Karli,[4] Florian Kappe,[4] Vikas Remesh,[4] Gregor Weihs,[4] Vollrath Martin Axt,[3] and Doris E. Reiter[2]

[1]*Institut für Festkörpertheorie, Universität Münster, 48149 Münster, Germany*

[2]*Condensed Matter Theory, Department of Physics, TU Dortmund, 44221 Dortmund, Germany*

[3]*Theoretische Physik III, Universität Bayreuth, 95440 Bayreuth, Germany*

[4]*Institute für Experimentalphysik, Universität Innsbruck, Innsbruck, Austria*

(Received 7 September 2022; revised 19 December 2022; accepted 5 January 2023; published 23 January 2023)

To coherently control a few-level quantum emitter, typically pulses with an energy resonant to the transition energy are applied, making use of the Rabi mechanism, while a single off-resonant pulse does not result in a population inversion. Surprisingly, a two-color excitation with a combination of two off-resonant pulses is able to invert the system. In this paper, we provide an in-depth analysis of two-color excitation schemes within the dressed-state picture. We show that such schemes can be understood as a driving of the transition between the dressed states. In the two-level system this allows us to derive analytic expressions for the pulse parameters yielding a population inversion. We relate our findings to the Swing-UP of quantum EmitteR population (SUPER) mechanism, where the two pulses are red detuned. Our interpretation also holds in the case where one pulse is red detuned while the other pulse is blue detuned, as in dichromatic excitation schemes. We extend our considerations of the SUPER mechanism to the three-level system, where a strong mixing between the bare states takes place. The insights gained from these results help in finding accessible regimes for further experimental realizations of two-color excitation schemes.

DOI: 10.1103/PhysRevB.107.035425

I. INTRODUCTION

Extensive efforts are put into finding excitation protocols for quantum emitters, which can be used for the deterministic and efficient generation of single photons [1–23] or entangled photon pairs [24–48], both being essential building blocks in quantum information technology. While well-established schemes like resonant excitation, leading to Rabi rotations [49–51], or adiabatic rapid passage (ARP) [52–56] exist to excite a quantum emitter, to distinguish the emitted single photons from the excitation laser pulses one has to employ cross-polarization filtering, limiting the photon yield to 50% [57,58]. For quantum dots, several schemes have been introduced that circumvent this problem by allowing excitation using a detuned laser, like phonon-assisted preparation [59–62], spectrally shaped ARP [63], or excitation via the biexciton state [64]. The photon loss due to cross-polarization filtering can also be reduced by embedding the emitter in a suited photonic structure [65–68].

A radically different approach is the Swing-UP of quantum EmitteR population (SUPER) scheme [69–73] that exploits the coherence of the quantum system by using off-resonant and red-detuned pulse pairs. While SUPER uses two red-detuned pulses, excitation schemes based on one red- and one blue-detuned pulse, called dichromatic excitation schemes, have also been employed to invert the population [74–76]. The SUPER and dichromatic schemes therefore circumvent the necessity for polarization filtering, without relying on incoherent, or emitter-specific processes like phonon effects in a quantum dot, because the exciting laser frequency is energetically separated from the signal by several millielectronvolts.

In this paper we analyze the mechanism of a multipulse scheme in a dressed-state picture. The dressed states are the eigenstates of a coupled system-light Hamiltonian. Because the dressed-state description includes the system and its driving in a single picture, an in-depth understanding on how a specific scheme functions can be obtained [62,77,78]. We show how the dressed-state picture is applied to a multipulse scheme, where the pulses have different detunings with respect to the transition energy of the quantum emitter. We start with the SUPER scheme and then extend our considerations to dichromatic cases. The analysis allows us to find analytic expressions for the pulse parameters for optimal excitation in two-color excitations. For SUPER, we analyze a two-level system as well as the three-level exciton-biexciton system, which is commonly found in semiconductor quantum dots.

A. Dressed states

We start with a brief summary of the concept of dressed states for a general two-level system with the transition energy $\hbar\omega_0$ between the ground state $|g\rangle$ and an excited state $|x\rangle$, which is driven by an external source $\Omega(t) = \Omega_0(t)e^{-i\omega_L t}$ having a constant frequency ω_L and a time-dependent envelope $\Omega_0(t)$. This yields the standard Hamiltonian in the dipole- and rotating-wave approximations (RWA),

$$H_{\mathrm{TLS}} = \hbar\omega_0|x\rangle\langle x| - \frac{\hbar}{2}(\Omega(t)|x\rangle\langle g| + \mathrm{H.c.}). \tag{1}$$

*t.bracht@wwu.de

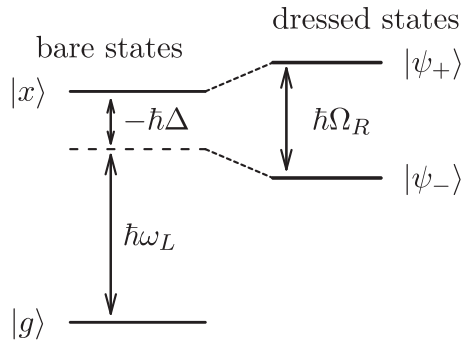

FIG. 1. Two-level system with ground state $|g\rangle$ and excited state $|x\rangle$, showing laser energy and detuning. In the dressed-state basis, the laser leads to an energy splitting with the Rabi energy.

Defining the detuning $\Delta = \omega_L - \omega_0$, the Hamiltonian can be rewritten in a rotating frame as

$$H_{\mathrm{TLS,RF}} = -\hbar\Delta|x\rangle\langle x| - \frac{\hbar}{2}(\Omega_0(t)|x\rangle\langle g| + \mathrm{H.c.}). \tag{2}$$

The term *dressed states* refers to the bare states $|g\rangle, |x\rangle$ that are *dressed* with the light field. They are calculated by diagonalizing the bare-state Hamiltonian and the electron-light interaction Hamiltonian. For constant fields, this is commonly done [79], while for time-dependent fields the transformation is performed for each point in time.

Diagonalizing the Hamiltonian in Eq. (2) results in

$$\tilde{H}_{\mathrm{TLS}} = E_+|\psi_+\rangle\langle\psi_+| + E_-|\psi_-\rangle\langle\psi_-|, \tag{3}$$

with the dressed states $|\psi_\pm\rangle$ and the dressed-state energies $E_\pm$,

$$E_\pm = \frac{\hbar}{2}\left(-\Delta \pm \sqrt{\Omega_0^2(t) + \Delta^2}\right), \tag{4}$$

with their difference being the Rabi splitting,

$$E_+ - E_- = \hbar\Omega_R(t) = \hbar\sqrt{\Omega_0^2(t) + \Delta^2}. \tag{5}$$

The splitting of the dressed-state energies in relation to the bare-state energies is schematically shown in Fig. 1.

The dressed states can be written as superpositions of the bare states:

$$\begin{aligned} |\psi_+\rangle &= c(t)|x\rangle - \tilde{c}(t)|g\rangle, \\ |\psi_-\rangle &= \tilde{c}(t)|x\rangle + c(t)|g\rangle, \end{aligned} \tag{6}$$

with the coefficients

$$\begin{aligned} c(t) &= \frac{\Omega_R(t) - \Delta}{\sqrt{\Omega_0^2(t) + (\Omega_R(t) - \Delta)^2}}, \\ \tilde{c}(t) &= \sqrt{1 - c^2(t)}. \end{aligned} \tag{7}$$

Other than in the bare-state picture, where $|g\rangle, |x\rangle$ are time independent, in the dressed-state picture the time dependence of the driving is accounted for by the state mixing and the dressed-state energies $E_\pm$.

B. Idea of SUPER

The concept behind the SUPER scheme, as it was proposed in Ref. [69], relies on the usage of two detuned pulses to drive a transition in a few-level system. The two laser frequencies lead to a beating effect, giving rise to changes in the excited-state population. Assuming that the system is initially in the ground state and the pulse parameters are tuned correctly, the system experiences a swing-up effect and ends up in the excited state. The multicolor pulse pair is described by

$$\Omega_X(t) = \Omega_1(t)e^{-i\omega_1 t} + \Omega_2(t)e^{-i\omega_2 t}. \tag{8}$$

Here, ω_j are the central frequencies of the pulses and $\Omega_j(t)$ are the (real) pulse envelopes. Note that the pulses do not have to fulfill a strict phase relationship, as shown in Ref. [69]. Phonons are known to result in decoherence effects for state preparation schemes in quantum dots [80], and the dot-phonon coupling exhibits a nonmonotonic behavior as a function of energy [81]. Accordingly, for high detuning and strong driving (as mostly considered in this manuscript), one is in the regime where the phonon influence is negligible, while it might become strong for small detuning and/or weak driving [71]. In order to focus on the interpretation of the dressed states, we neglect phonons in this paper and leave the discussion of dissipation for future work.

Essential properties of the laser pulses are their respective detunings to the transition frequency of the quantum emitter ω_0, defined as

$$\Delta_j = \omega_j - \omega_0. \tag{9}$$

In the following we will refer to the two pulses by the "first" pulse with detuning Δ_1 and the "second" pulse with detuning Δ_2. This naming convention refers to the idea that the parameters for the first pulse are fixed and determine the parameters of the second pulse. Hence, the naming shall not necessarily indicate a temporal order. We remind the reader that the two pulses should overlap in time for SUPER to work. Most importantly, it was shown in Ref. [69] that the frequency difference of the pulses should coincide with the Rabi frequency induced by the first pulse. This means the pulse energies cannot be chosen arbitrarily but have a fixed relation to each other. In the following, we show how this relation can be extracted from the dressed-state picture.

II. DRESSED STATE ANALYSIS OF A TWO-LEVEL SYSTEM

We begin the study of the influence of the multicolor pulses on a two-level system by replacing the single laser pulse in Eq. (1) with the multicolor pulse as defined in Eq. (8), within the Hamiltonian

$$H = \hbar\omega_0|x\rangle\langle x| - \frac{\hbar}{2}(\Omega_X(t)|x\rangle\langle g| + \mathrm{H.c.}). \tag{10}$$

Because the Hamiltonian now contains two laser frequencies, the transformation into the rotating frame is somewhat ambiguous, as several frequencies can be chosen. We decide to transform the Hamiltonian in Eq. (10) to a reference frame rotating with frequency ω_1 of the first pulse, yielding

$$\begin{aligned} H_{RF} =& -\hbar\Delta_1|x\rangle\langle x| - \frac{\hbar}{2}\Omega_1(t)(|x\rangle\langle g| + |g\rangle\langle x|) \\ & - \frac{\hbar}{2}\Omega_2(t)(e^{i\omega_\Delta t}|x\rangle\langle g| + e^{-i\omega_\Delta t}|g\rangle\langle x|) \\ =& H_0 + H_{\Omega_1} + H_{\Omega_2}. \end{aligned} \tag{11}$$

After the rotating frame transformation, $H_0 + H_{\Omega_1}$ is purely real, while H_{Ω_2} still includes terms oscillating with the frequency difference between the two pulses, which we define as

$$\omega_\Delta = \omega_1 - \omega_2 = \Delta_1 - \Delta_2. \tag{12}$$

Note that ω_Δ is a difference of two frequencies and can take on negative values.

A. Dressed states including the first pulse

To analyze the energetic splitting induced by the first pulse, a transformation to a dressed-state basis is performed, including only the first pulse and neglecting the second pulse for now. In some sense, these are partially dressed states. In other words, we diagonalize $H_0 + H_{\Omega_1}$ in Eq. (11), leading to the energies and states as given in Eqs. (4) and (6).

For illustrative purposes, let us consider a system where these partially dressed states are approximately time independent. We achieve this by assuming a rectangular-shaped pulse, though such pulses are challenging to realize with state-of-the-art laser systems [82]. To avoid instantaneous switching of the pulse that leads to many additional components in the laser spectrum and to allow for dressing and undressing processes [62], we consider a switch on/off process of finite duration. This is modeled using two Sigmoid-type functions to assure smooth edges:

$$\Omega_1(t) = \frac{\Omega_1^{\text{rect}}}{(1 + e^{-\kappa(\tau/2+t)})(1 + e^{-\kappa(\tau/2-t)})}. \tag{13}$$

This pulse has an approximate plateau duration of τ, while κ determines the duration of the pulse edges. Ω_1^{rect} is a measure for the amplitude of the pulse during its *on* state. During the plateau region of the pulse, the dressed states are essentially constant, such that we do not have to account for the time dependence of the dressed-state quantities. Noticeable changes only happen during the dressing and undressing process.

As parameters we choose a detuning of $\hbar\Delta_1 = -5\,\text{meV}$ and an amplitude of $\hbar\Omega_1^{\text{rect}} = 4\,\text{meV}$. These parameters are typical when dealing with the optical excitation of quantum dots, and the excited-state lifetime is about an order of magnitude larger than the pulse duration. Figure 2(a) shows the dressed-state energies for this rectangular pulse shape with $\tau = 40\,\text{ps}$ and $\kappa = 1\,\text{ps}^{-1}$. Before and after the pulse, the energies are split by the detuning $\hbar\Delta_1$ of the laser due to the frame of reference. During the pulse, the branches shift apart by a constant splitting of 6.4 meV, as described by Eq. (5). Before and after the pulse, the upper dressed state $|\psi_+\rangle$ can be identified with the excited state $|x\rangle$, while the lower dressed state $|\psi_-\rangle$ can be identified with the ground state $|g\rangle$.

B. Transformation of the second pulse

In the next step we study the influence of the second pulse, interacting with the system at the same time as the first pulse. Correspondingly, the interaction Hamiltonian $\tilde{H}_{\Omega_2}$ is transformed to the dressed-state picture of the first pulse. The inverse transformation to Eq. (6) leads to the transformed

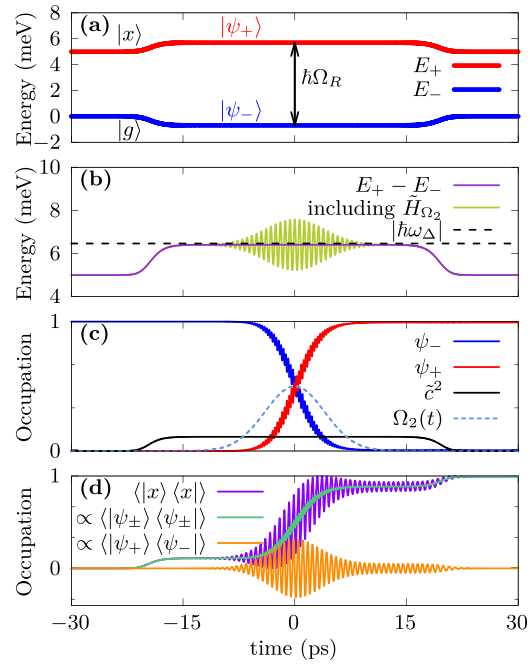

FIG. 2. Time evolution of several quantities: (a) Energies of the dressed states for a rectangular pulse with smoothened edges with $\hbar\Delta_1 = -5\,\text{meV}$, $\tau = 40\,\text{ps}$, $\kappa = 1\,\text{ps}^{-1}$, $\hbar\Omega_0 = 4\,\text{meV}$. (b) Energy difference of upper and lower dressed state excluding (violet) and including (green) the influence of the second pulse. The dashed black line indicates the detuning of the second pulse, which in the rotating frame is $|\hbar\omega_\Delta|$. (c) Dressed-state occupation under the second pulse with $\sigma_2 = 4\,\text{ps}$, $\alpha_2 = 9.13\pi$, $\hbar\Delta_2 = -11.46\,\text{meV}$, where the second pulse is indicated by the dashed line. (d) Occupation of the excited state in the bare-state picture as well as contributions of the dressed states.

Hamiltonian:

$$\tilde{H}_{\Omega_2} = \hbar\Omega_2(t)c\tilde{c}\,\cos(\omega_\Delta t)(|\psi_+\rangle\langle\psi_+| - |\psi_-\rangle\langle\psi_-|) - \frac{\hbar}{2}\Omega_2(t)[(c^2 e^{i\omega_\Delta t} - \tilde{c}^2 e^{-i\omega_\Delta t})|\psi_+\rangle\langle\psi_-| + \text{H.c.}]. \tag{14}$$

On one hand, the Hamiltonian $\tilde{H}_{\Omega_2}$ leads to additional energy shifts due to the $|\psi_\pm\rangle\langle\psi_\pm|$ terms. These energy shifts cause an oscillation of the dressed-state energies $E_\pm$,

$$E_\pm \to E_{\pm,2} = E_\pm \pm \hbar\Omega_2(t)c\tilde{c}\cos(\omega_\Delta t). \tag{15}$$

On the other hand, $\tilde{H}_{\Omega_2}$ also leads to transitions between the dressed states, mediated by the $|\psi_\pm\rangle\langle\psi_\mp|$ terms. The term $\propto c^2 e^{i\omega_\Delta t}$ as well as the term $\propto \tilde{c}^2 e^{-i\omega_\Delta t}$ in Eq. (14) drives these transitions. In analogy to the usual two-level system, we arrive at

$$\tilde{H} = E_{+,2}|\psi_+\rangle\langle\psi_+| + E_{-,2}|\psi_-\rangle\langle\psi_-| - \frac{\hbar}{2}\Omega_2(t)[(c^2 e^{i\omega_\Delta t} + \tilde{c}^2 e^{-i\omega_\Delta t + i\pi})|\psi_+\rangle\langle\psi_-| + \text{H.c.}]. \tag{16}$$

This resembles the Hamiltonian of a two-level system, consisting of the two states $|\psi_+\rangle$, $|\psi_-\rangle$, driven by the second laser

pulse, while the driving $\Omega_2(t)$ is modified by the dressed-state coefficients. An interesting aspect is that it contains both the positive and the negative frequency component $e^{\pm i\omega_\Delta t}$. This is in analogy to a Hamiltonian where the RWA has not been performed. We remember that in the RWA for the raising operator $|\psi_+\rangle\langle\psi_-|$ only terms with $e^{-i|\omega|t}$ are considered. However, because ω_Δ can take positive and negative values, both terms are important in Eq. (16). We distinguish two cases: (i) driving based on $e^{-i\omega_\Delta t+i\pi}$, where the additional phase of π will be neglected in the following, and (ii) driving based on $e^{+i\omega_\Delta t}$.

For now, we focus on case (i). Similar to a standard two-level system, the raising operation $\propto e^{-i\omega_\Delta t}$ is resonant if the frequency $\omega_\Delta > 0$ corresponds to the energy difference of the two levels, that is,

$$\hbar\omega_\Delta = E_{+,2} - E_{-,2} = E_+ - E_- + 2\hbar\Omega_2(t)c\tilde{c}\cos(\omega_\Delta t). \quad (17)$$

However, this energy difference is time dependent and depends on ω_Δ itself. In order to find the resonance condition for the second pulse, we take the mean energy difference, neglecting the fast oscillations of the dressed-state energies. Using Eq. (12), this gives us the condition for the detuning of the second pulse with

$$\begin{aligned}\omega_\Delta &= (E_+ - E_-)/\hbar = \Omega_R = \sqrt{\left(\Omega_1^{\mathrm{rect}}\right)^2 + \Delta_1^2} \\ &\Rightarrow \Delta_2 = \Delta_1 - \Omega_R. \end{aligned} \quad (18)$$

In this configuration, the second laser pulse is always energetically below the first one.

C. Driving the dressed two-level system

Keeping these results in mind, we now consider the scenario shown in Fig. 2(a) and search for a second pulse to excite the system. For the second pulse, we use a Gaussian pulse envelope given by

$$\Omega_2(t) = \frac{\alpha_2}{\sqrt{2\pi}\sigma_2} e^{-\frac{t^2}{2\sigma_2^2}}, \quad (19)$$

with pulse area α_2 and duration σ_2. The duration of the second pulse has to be chosen such that it lies completely inside the plateau region of the first pulse.

In analogy with the bare-state two-level system, we now search for a pulse, which results in an inversion between the dressed states, i.e., which transfers the system completely from its initial state $|\psi_-\rangle$ to $|\psi_+\rangle$. In other words, a π rotation has to be performed in the dressed-state picture. Looking at the Hamiltonian in Eq. (16), the pulse area (and Rabi frequency) of the second pulse is effectively reduced by the factor $\tilde{c}^2$. Due to this renormalization of the pulse area, α_2 has to be scaled by this factor such that $\tilde{c}^2\alpha_2 = \pi$, yielding the condition

$$\alpha_2 = \frac{\pi}{\tilde{c}^2}. \quad (20)$$

Here we use $\sigma_2 = 4\,\mathrm{ps}$. We choose the detuning of the second pulse to be smaller than the first one, i.e., using the raising operation $\propto e^{-i\omega_\Delta t}$ with $\omega_\Delta > 0$.

1. Negative Δ_1

As the first pulse has a negative detuning of $\hbar\Delta_1 = -5\,\mathrm{meV}$, both exciting lasers are below the excited-state transition. From Eq. (18) using $\hbar\Omega_R = 6.4\,\mathrm{meV}$, we calculate a detuning of $\hbar\Delta_2 = -11.4\,\mathrm{meV}$ for the second pulse. The necessary pulse area follows from Eq. (20) and evaluates to $\alpha_2 \approx 9.13\pi$. We stress that the first pulse completely determines the properties of the second pulse needed to perform a rotation in the dressed-state basis.

Figure 2 shows the effect of this second pulse on the system. In Fig. 2(b), the energy difference of the dressed states is shown in violet, while the green line includes the contributions of the second pulse. This leads to the additional oscillatory splitting of the dressed states described in Eq. (15). The black dashed line indicates the energy of the second laser.

For Δ_2, we determined numerically that an additional shift of about $-0.06\,\mathrm{meV}$ is needed to reach optimal excitation, i.e., $\hbar\Delta_2 = -11.46\,\mathrm{meV}$, which we attribute to perturbations due to the strong second pulse. In Fig. 2(c) the time evolution of the dressed-state occupation is shown alongside the coupling $\tilde{c}^2$ and the second laser envelope (normalized). The dressed-state occupation performs a Rabi-like oscillation from $|\psi_-\rangle$ to $|\psi_+\rangle$. During the rise of the dressed-state occupation, the occupation displays an additional low-amplitude high-frequency oscillation. The latter can be associated with the additional oscillations in the energy difference $E_{+,2} - E_{-,2}$ [see panel (b)].

Figure 2(d) shows the time evolution of the excited-state population in purple. As intended, the occupation inverts during the action of both pulses from the ground to its excited state. The main rise is during the action of the second pulse, where also in the dressed-state picture, the second pulse mimicks a π pulse that inverts the states. In addition, at the smoothened edges of the first pulse, a rise of the excited-state occupation of the magnitude of the state mixing of $\tilde{c}^2 = 0.11$ takes place. This adiabatic dressing and undressing effect is needed to fully invert the system, as has already been discussed for phonon-assisted state preparation schemes for excitons in quantum dots [62]. Hence, better results are obtained for smooth pulses such as Eq. (13), in contrast to sharp rectangular ones.

The dressed-state picture can also be used for an even deeper analysis by separating the fast, high-amplitude oscillations in the bare states from the mean rise of the occupation. Expressing the excited-state occupation in terms of the dressed states reads

$$\begin{aligned}\langle|x\rangle\langle x|\rangle = {} & c^2\langle|\psi_+\rangle\langle\psi_+|\rangle + \tilde{c}^2\langle|\psi_-\rangle\langle\psi_-|\rangle \\ & + 2c\tilde{c}\,\mathrm{Re}(\langle|\psi_+\rangle\langle\psi_-|\rangle). \end{aligned} \quad (21)$$

Here, the first line of Eq. (21) can be interpreted as the contribution of the dressed-state population to the bare-state occupations due to mixing. The part in the second line depends on the term $\langle|\psi_+\rangle\langle\psi_-|\rangle$, which represents the coherence between the dressed states. This coherence builds up with the second pulse and, similar to the coherence $\langle|g\rangle\langle x|\rangle$ between the bare states, gives rise to transitions between the dressed states. However, additionally, it leads to a contribution to the bare-state occupation. A sizable influence of this term is the fingerprint of a nonadiabatic time evolution.

Both parts contributing to $\langle|x\rangle\langle x|\rangle$ are shown in Fig. 2(d). Comparing the two different contributions (green for population contribution and orange for the coherence contribution) to

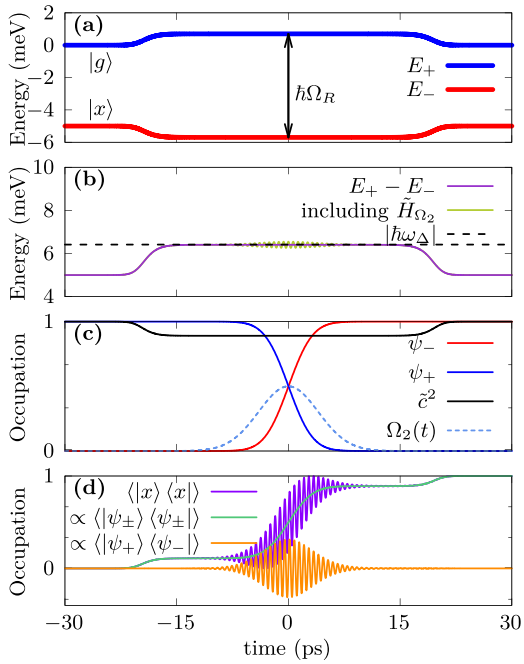

FIG. 3. Same as Fig. 2 but for a positive detuning of $\hbar\Delta_1 = +5\,\text{meV}$, which yields as parameters for the second pulse $\sigma_2 = 4\,\text{ps}$, $\alpha_2 = 1.12\pi$, $\hbar\Delta_2 = -1.41\,\text{meV}$.

the exciton occupation $\langle|x\rangle\langle x|\rangle$, we see that the mean behavior of the exciton occupation is determined by the population contribution. This holds in particular for the rise during the second pulse and the adiabatic dressing and undressing effects at the smoothened edges of the pulse. The coherence contribution starts during the second pulse and features a large-amplitude oscillation, which is also clearly visible in the excited-state occupation.

2. Positive Δ_1

So far, we focused on the case where both pulses are tuned below the excited-state energy. However, Eq. (18) also holds for positive Δ_1 (and still $\omega_\Delta > 0$). Such cases were not considered in the SUPER proposal [69] but were addressed in dichromatic excitation schemes [74–76].

Choosing the same shape of the first pulse as before, but using $\hbar\Delta_1 = +5\,\text{meV}$, leads to the dressed-state energies shown in Fig. 3(a). Now, before and after the pulse, the upper dressed state corresponds to the ground state and the lower dressed state corresponds to the excited state. This means that c and $\tilde{c}$ change roles, i.e., now $\tilde{c}^2 = 0.89$. With these parameters and a splitting of the dressed states of $\hbar\Omega_R = 6.4\,\text{meV}$, according to Eq. (18) the energy of the second pulse evaluates to $\hbar\Delta_2 = -1.413\,\text{meV}$, which also agrees with the numerically found optimal parameters. The necessary pulse area evaluates to only $\alpha_2 = 1.12\pi$, as the coupling coefficient $\tilde{c}^2$ is large [cf., Fig. 3(c)]. Energetically, this also leads to a lower impact of the second pulse on the dressed-state energies, such that it is resonant with the dressed-state transition for most of the time, even during the time it leads to an additional shift [see green line in Fig. 3(b)]. Figure 3(d) shows the exciton population, and the dressed-state contributions, where both the dressed-state occupation and the coherences contribute to the behavior of the bare-state occupation. Again, the dressed-state picture provides a very useful analytic expression, yielding parameters that lead to a complete occupation of the excited state.

We relate our findings to the dichromatic excitation schemes [74,75], which have been experimentally realized. In these cases small detunings were used, such that strong pulses lead to cases which appear almost symmetric in the detuning. In fact, in Ref. [75] it was discussed that totally symmetric excitation pulses do not lead to an occupation. Our predictions of the used detunings also agree well with parameters suggested in Ref. [76], where in the theoretical curves also clearly a swing-up dynamics is observed. Hence, the interpretation within the dressed-state picture can be applied to both types of two-color excitation schemes, SUPER and dichromatic.

TABLE I. Detunings used for Figs. 2 and 3, also showing the combinations of detunings, when the second possible raising operation in Eq. (16) is used. We note that the explicit detunings depend on the pulse strength.

$\hbar\Delta_2$ for	$\hbar\Delta_1 = -5\,\text{meV}$	$\Delta_1 = 5\,\text{meV}$
$\omega_\Delta > 0$	$-11.46\,\text{meV}$ (Fig. 2)	$-1.41\,\text{meV}$ (Fig. 3)
$\omega_\Delta < 0$	$1.41\,\text{meV}$	$11.46\,\text{meV}$

3. Negative ω_Δ

We remind the reader that Eq. (16) includes two possible cases for ω_Δ that lead to transitions. The second possible raising operation, $\propto e^{i\omega_\Delta t}$, is resonantly driven if we account for the opposite sign, i.e., the energetic condition changes to $-\hbar\omega_\Delta = E_{+,2} - E_{-,2}$. This is in agreement with ω_Δ being able to take negative values and leads to a symmetry in the possible detunings, which is shown in Table I. The signs of both detunings can be switched at the same time, under which the dynamics stay the same, except for a constant phase. Note that possible environmental effects, such as electron-phonon interaction in quantum dots, are not symmetric with respect to the detuning.

D. Gaussian pulses

In the proposal [69] as well as in the experimental realization [72], two Gaussian pulses were used, such that also for the first pulse we now take a Gaussian envelope

$$\Omega_1(t) = \frac{\alpha_1}{\sqrt{2\pi}\sigma_1} e^{-\frac{t^2}{2\sigma_1^2}}, \tag{22}$$

with the parameter set of Ref. [69] with $\sigma_1 = 2.4\,\text{ps}$, $\hbar\Delta_1 = -8\,\text{meV}$, $\alpha_1 = 22.65\pi$. The resulting dressed-state energies are shown in Fig. 4(a). During the pulse, the branches split by up to 11.163 meV. Using this maximum splitting in Eq. (18) leads to $\hbar\Delta_2 = -19.163\,\text{meV}$, the value also used in the original paper. Here, at the maximum of the first pulse, $\tilde{c}^2 = 0.145$. But due to the continuous change in both pulse envelopes, the condition for the pulse area α_2 as in Eq. (20) cannot be applied.

The energy difference of the dressed states is displayed in Fig. 4(b). The violet line depicts the energy difference of the

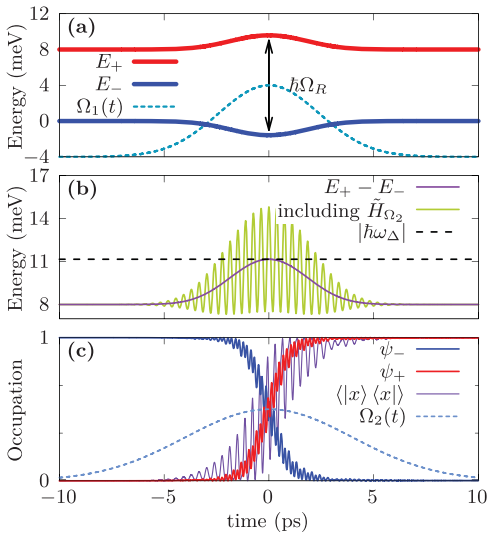

FIG. 4. (a) Dressed-state energies $E_\pm$ induced by a single off-resonant Gaussian pulse, $\sigma_1 = 2.4\,\text{ps}$, $\hbar\Delta_1 = -8\,\text{meV}$, $\alpha_1 = 22.65\pi$, as indicated by the dashed line. (b) Energy difference of the dressed states, (violet) without and (green) including the interaction Hamiltonian $\tilde{H}_{\Omega_2}$ (second pulse parameters: $\sigma_2 = 3.04\,\text{ps}$, $\hbar\Delta_2 = -19.163\,\text{meV}$, $\alpha_2 = 19.29\pi$). The dashed black line depicts the energy of the second laser. (c) Dressed-state and excited-state occupation. The dashed blue line shows the shape of the second pulse.

two dressed states without the interaction Hamiltonian $\tilde{H}_{\Omega_2}$. When the additional energy shifts due to $\tilde{H}_{\Omega_2}$ are included, the oscillations according to Eq. (14) can be observed, shown as the green line. The dashed black line, marking the energy of the second laser in this rotating frame, crosses the green line several times. As soon as the energy matches, the dressed-state occupation starts to switch significantly from $|\psi_-\rangle$ to $|\psi_+\rangle$, as visible in Fig. 4(c). The oscillating energy difference again leads to an oscillation in the dressed-state occupation as well. Although the second pulse is longer than the first one, the dynamics only happens in the time interval in which the energy-matching condition is fulfilled, which means where the first pulse splits the dressed states. This is in accordance with the observation that a single, highly detuned pulse does not lead to transitions in a simple two-level system, but the pulse pair is able to switch the occupation from the ground to the excited state.

III. THREE-LEVEL SYSTEM

Quantum dots can be used to generate entangled photons via the biexciton-exciton cascade. For this, a deterministic and high-fidelity preparation of the biexciton state $|xx\rangle$ is required. Therefore here we analyze, within the dressed-state picture, how this can be achieved with two red-detuned pulses as used in SUPER.

Assuming linear polarization of the laser, the Hamiltonian including the biexciton can be written as a three-level system by adding the biexciton state $|xx\rangle$:

$$H = \hbar\omega_0|x\rangle\langle x| + \hbar(2\omega_0 - \Delta_B)|xx\rangle\langle xx| - \frac{\hbar}{2}[\Omega_X(t)(|x\rangle\langle g| + |xx\rangle\langle x|) + \text{H.c.}]. \quad (23)$$

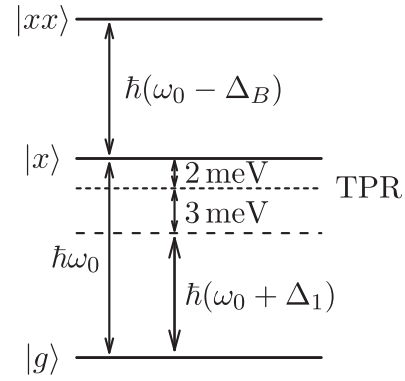

FIG. 5. Three-level system with ground state $|g\rangle$, exciton state $|x\rangle$, and biexciton state $|xx\rangle$. The detuning of the first laser is tuned 3 meV below the two-photon resonance (TPR), which is located at $-2\,\text{meV}$.

The energy of the biexciton is decreased by the binding energy $\hbar\Delta_B$ compared to double the exciton energy $\hbar\omega_0$. We set $\hbar\Delta_B = 4\,\text{meV}$, which is typical for quantum dots used in recent experiments [72].

Following the procedure from the two-level system, a transformation to a reference frame rotating with the frequency of the first laser leads to

$$\begin{aligned} H_{RF} =& -\hbar\Delta_1|x\rangle\langle x| - \hbar(2\Delta_1 + \Delta_B)|xx\rangle\langle xx| \\ &- \frac{\hbar}{2}\Omega_1(t)[(|x\rangle\langle g| + |xx\rangle\langle x|) + \text{H.c.}] \\ &- \frac{\hbar}{2}\Omega_2(t)[e^{i\omega_\Delta t}(|x\rangle\langle g| + |xx\rangle\langle x|) + \text{H.c.}] \\ =& H_0 + H_{\Omega_1} + H_{\Omega_2}. \end{aligned} \quad (24)$$

A. Effect of the first pulse

Again, the Hamiltonian $H_0 + H_{\Omega_1}$ is diagonalized to arrive at the dressed-state picture, now consisting of the three dressed states:

$$|\psi_j(t)\rangle = \sum_{k\in\{g,x,xx\}} a_{j,k}(t)|k\rangle, \quad j = 1, 2, 3, \quad (25)$$

at the energies E_j. The coefficients $a_{j,k}(t)$ of the bare states are determined numerically. For a first laser pulse with a detuning of $\hbar\Delta_1 = -5\,\text{meV}$ to the exciton transition, the laser is red detuned to the two-photon resonance by $-3\,\text{meV}$, as shown schematically in Fig. 5. For a pulse with $\alpha_1 = 27\pi$ and $\sigma_1 = 3\,\text{ps}$, the dressed-state energies are shown in Fig. 6(a). The three dressed states can be identified with the ground, exciton, and biexciton state before and after the pulse. During the pulse, the energy branches bent in such a way that there is a splitting of 12.31 meV between E_3 and E_1. The middle branch bends downward, yielding an energy separation of 5.88 meV between E_2 and E_1. The color of the branches in Fig. 6(a) indicates the mixing of the states. We find that in particular the mixing between $|x\rangle$ and $|xx\rangle$ is strong. For example, at $t = 0$ the state $|\psi_2\rangle$, having the middle energy, consists of 26.4 % $|g\rangle$, 23.2 % $|x\rangle$, and 50.4 % $|xx\rangle$, i.e., the middle branch consists of >50 % $|xx\rangle$ at the peak of the first pulse, while it corresponds to $|x\rangle$ before and after the pulse. Having in mind that the goal is to excite either the exciton or the biexciton,

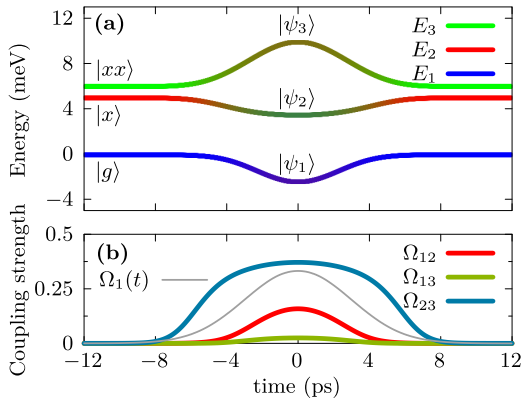

FIG. 6. (a) Dressed-state energies $E_{1,2,3}$ for the biexciton system interacting with a single off-resonant pulse, $\sigma_1 = 3\,\mathrm{ps}$, $\hbar\Delta_1 = -5\,\mathrm{meV}$, $\alpha_1 = 27\pi$. The color indicates how the dressed states mix from the bare states. (b) Coupling coefficients given in Eq. (27), corresponding to the pulse in (a) as well as the laser envelope (arb. units). The time interval as well as the strength of the coupling is different for all three possible transitions, with the $|\psi_2\rangle \leftrightarrow |\psi_3\rangle$ transition showing by far the strongest coupling.

it is desirable to find a second laser which induces transitions between the dressed states $|\psi_{1,2,3}\rangle$.

B. Driving the dressed states

To gain more insight into the transitions between the dressed states, the Hamiltonian of the system is transformed to the dressed-state basis. Similar to Eq. (14), the interaction Hamiltonian $\tilde{H}_{\Omega_2}$ in the biexciton system not only results in additional energy contributions to the dressed states, which lead to the oscillatory behavior visible in Figs. 7(a) and 8(a),

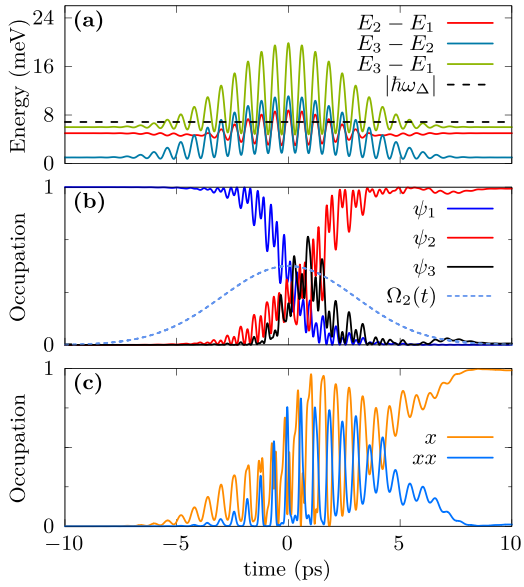

FIG. 7. (a) Energy differences of the dressed states including the interaction Hamiltonian $\tilde{H}_{\Omega_2}$ containing a pulse with $\sigma_2 = 3\,\mathrm{ps}$, $\hbar\Delta_2 = -11.83\,\mathrm{meV}$, $\alpha_2 = 22.8\pi$. The black dashed line depicts the energy of the second laser in this frame of reference. (b) Dressed-state occupations. The dashed blue line indicates the second pulse. (c) Occupation of exciton and biexciton.

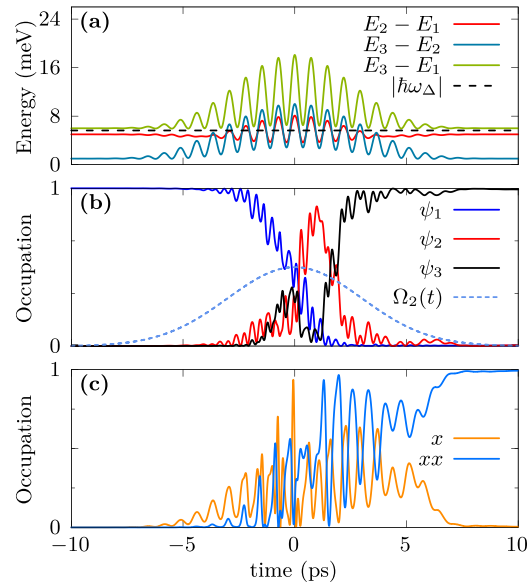

FIG. 8. Same as Fig. 7 but addressing the biexciton. For this, the detuning and pulse area of the second pulse are changed to $\hbar\Delta_2 = -10.64\,\mathrm{meV}$, $\alpha_2 = 17.49\pi$.

but also to a coupling of the dressed states. Here we only want to consider the terms $\propto |\psi_j\rangle\langle\psi_k| e^{-i\omega_\Delta t}$ with $\omega_\Delta > 0$ for $j > k$ (i.e., $|\psi_j\rangle\langle\psi_k|$ corresponds to a raising operator), which always leads to transitions driven by $\Delta_2 < \Delta_1$. In principle, resonances between two dressed states $|\psi_j\rangle$, $|\psi_k\rangle$ can be accessed with Δ_2 according to

$$\begin{aligned} \omega_\Delta &= \Delta E_{jk}/\hbar \\ &\Rightarrow \Delta_2 = \Delta_1 - \Delta E_{jk}/\hbar. \end{aligned} \tag{26}$$

Here, ΔE_{jk} is the energy difference between two of the dressed states. In principle, the condition can be chosen to $\hbar\omega_\Delta = \Delta E_{21}$ or $\hbar\omega_\Delta = \Delta E_{32}$, but the strong state mixing prevents a clear final state as discussed below. In the transformed Hamiltonian $\tilde{H}_{\Omega_2}$, the coupling terms $\propto e^{-i\omega_\Delta t}$ of the second laser are

$$\begin{aligned} \tilde{H}_{\Omega_2} = -\frac{\hbar\Omega_2}{2} e^{-i\omega_\Delta t} \Big[& \underbrace{(a_{2,g}a_{1,x} + a_{2,x}a_{1,xx})}_{:=\Omega_{12}(t)} |\psi_2\rangle\langle\psi_1| \\ & \times \underbrace{(a_{3,g}a_{1,x} + a_{3,x}a_{1,xx})}_{:=\Omega_{13}(t)} |\psi_3\rangle\langle\psi_1| \\ & \times \underbrace{(a_{3,g}a_{2,x} + a_{3,x}a_{2,xx})}_{:=\Omega_{23}(t)} |\psi_3\rangle\langle\psi_2| \Big] + \mathrm{H.c.} + \cdots . \end{aligned} \tag{27}$$

While in the bare-state picture the laser has the same coupling element for the $|g\rangle \leftrightarrow |x\rangle$ and $|x\rangle \leftrightarrow |xx\rangle$ transitions, in this picture there are different coupling terms Ω_{jk} for direct transitions between the dressed states $|\psi_j\rangle$ and $|\psi_k\rangle$.

Figure 6(b) shows the time-dependent coupling coefficients given in Eq. (27) for the first pulse chosen in Fig. 6(a). The couplings of the three possible transitions show significant differences, with Ω_{23} extending over the longest time period and having the largest amplitude. The transition coupled with Ω_{12} shows about half the coupling strength, while

Ω_{13} only leads to a weak direct coupling of states $|\psi_1\rangle$ and $|\psi_3\rangle$.

Due to these simultaneous transitions between the dressed states, no clear criteria for high excitation of the exciton or biexciton state using a second pulse follows from this picture, so Eq. (26) cannot be used, and we performed a numerical parameter search.

1. Exciton preparation

To excite the exciton, the dressed state $|\psi_2\rangle$ has to be populated by a second pulse, since this state evolves into $|x\rangle$ in the adiabatic undressing process. We use the same first pulse as in Fig. 6(a). Numerical searching for parameters leads to a second pulse with $\sigma_2 = 3\,\mathrm{ps}$, $\hbar\Delta_2 = -11.83\,\mathrm{meV}$, $\alpha_2 = 22.8\pi$. Figure 7(a) shows the energy separation of the dressed states, including the effect of the second pulse. The strong second laser leads to a high-amplitude oscillation of the dressed-state energies, such that the energy of the second laser (depicted as the black dashed line) overlaps with the energy differences of the dressed states in a prolonged time window. Panel (b) shows the dressed-state occupations. Similarly to the case of the two-level system, the occupation is transferred between the dressed states in an oscillatory fashion. However, the transfer starts only after the laser energy matches the splitting of the dressed states and can drive the transitions $|\psi_1\rangle \leftrightarrow |\psi_2\rangle$ and $|\psi_2\rangle \leftrightarrow |\psi_3\rangle$. While the energy also matches the $|\psi_1\rangle \leftrightarrow |\psi_3\rangle$ transition, this transition is strongly suppressed, as was shown in Fig. 6(b). Nevertheless, $|\psi_3\rangle$ is populated during the dynamics due to the stronger $|\psi_2\rangle \leftrightarrow |\psi_3\rangle$ coupling. With the selected parameters, the occupation switches to the dressed state $|\psi_2\rangle$, which after the pulses corresponds to the exciton state. The bare-state populations [panel (c)] show that during the pulses, both the exciton and biexciton state are addressed by the process, before the population switches to the exciton state.

2. Biexciton preparation

Next, we analyze the dressed-state dynamics for a second pulse that results in complete population transfer to the biexciton state. The first pulse is the same as used before, only the detuning and pulse parameters of the second pulse are changed to $\hbar\Delta_2 = -10.64\,\mathrm{meV}$ and $\alpha_2 = 17.49\pi$. The dressed-state analysis for this case is shown in Fig. 8. Now, the second detuning is slightly lower than in the previous case, so in panel (a) the energy of the second laser (black dashed line) does not cross the energy difference $E_3 - E_1$ anymore but lies more centrally towards the energies needed for the $|\psi_1\rangle \leftrightarrow |\psi_2\rangle$ and $|\psi_2\rangle \leftrightarrow |\psi_3\rangle$ transitions. Looking at the dressed-state occupations in panel (b), the occupation is first transferred from $|\psi_1\rangle$ to $|\psi_2\rangle$, similar to the previous case. Subsequently, the occupation is fully transferred to the dressed state $|\psi_3\rangle$. After the undressing resulting from smoothly switching off the pulse, this corresponds to the biexciton state. Accordingly, in Fig. 8(c) we see that during the pulse again both the exciton and biexciton are addressed, while after the pulse only the biexciton is populated.

As such, the scheme can also be used to off-resonantly excite the biexciton, which of course is also possible using two-photon resonant transitions [83]. However, it was shown recently that this hinders optimal entanglement generation [84], so other options to excite the biexciton can be beneficial in the future.

IV. CONCLUSION

In this work we analyzed the impact of two simultaneous laser pulses on a quantum emitter that are detuned to the transition energy. A red-detuned pulse pair is used in two-color excitation like the SUPER scheme, as proposed theoretically [69] and implemented for quantum dots [72] to populate the excited state in a two-level system. A pulse pair with a red- and a blue-detuned pulse has been used in dichromatic schemes [74–76].

Using the dressed-state picture, we find that choosing one pulse uniquely determines the optimal parameters for the other pulse. For the two-level system, we provide analytic formulas [see, for example, Eq. (18) together with Eq. (20)] for the second pulse for optimal preparation of the excited state. We have demonstrated that many combinations of positive and negative detunings can lead to an occupation of the excited state, leading to flexibility in the design of future experiments. Further, we discussed that in a three-level system, the two-pulse excitation can be used to selectively excite the exciton or biexciton. These results enable the operation of single-photon or entangled photon sources relying on two-color excitation schemes.

ACKNOWLEDGMENTS

T.K.B. and D.E.R. acknowledge financial support from the German Research Foundation DFG through project 428026575 (AEQuDot). F.K., Y.K., V.R. and G.W. acknowledge financial support through the Austrian Science Fund FWF projects W1259 (DK-ALM Atoms, Light, and Molecules), FG 5, TAI-556N (DarkEneT) and I4380 (AEQuDot).

[1] P. Michler, A. Kiraz, C. Becher, W. V. Schoenfeld, P. M. Petroff, L. Zhang, E. Hu, and A. Imamoğlu, A quantum dot single-photon turnstile device, Science **290**, 2282 (2000).

[2] C. Santori, M. Pelton, G. Solomon, Y. Dale, and Y. Yamamoto, Triggered Single Photons from a Quantum Dot, Phys. Rev. Lett. **86**, 1502 (2001).

[3] Y.-M. He, Y. He, Y.-J. Wei, D. Wu, M. Atatüre, C. Schneider, S. Höfling, M. Kamp, C.-Y. Lu, and J.-W. Pan, On-demand semiconductor single-photon source with near-unity indistinguishability, Nat. Nanotechnol. **8**, 213 (2013).

[4] Y.-J. Wei, Y.-M. He, M.-C. Chen, Y.-N. Hu, Y. He, D. Wu, C. Schneider, M. Kamp, S. Höfling, C.-Y. Lu *et al.*, Deterministic

and robust generation of single photons from a single quantum dot with 99.5% indistinguishability using adiabatic rapid passage, Nano Lett. **14**, 6515 (2014).

[5] P. Tonndorf, R. Schmidt, R. Schneider, J. Kern, M. Buscema, G. Steele, A. Castellanos-Gomez, H. van der Zant, S. Michaelis de Vasconcellos, and R. Bratschitsch, Single-photon emission from localized excitons in an atomically thin semiconductor, Optica **2**, 347 (2015).

[6] N. Somaschi, V. Giesz, L. De Santis, J. C. Loredo, M. P. Almeida, G. Hornecker, S. L. Portalupi, T. Grange, C. Antón, J. Demory, C. Gómez, I. Sagnes, N. D. Lanzillotti-Kimura, A. Lemaítre, A. Auffeves, A. G. White, L. Lanco, and P. Senellart, Near-optimal single-photon sources in the solid state, Nat. Photonics **10**, 340 (2016).

[7] X. Ding, Y. He, Z.-C. Duan, N. Gregersen, M.-C. Chen, S. Unsleber, S. Maier, C. Schneider, M. Kamp, S. Höfling, C.-Y. Lu, and J.-W. Pan, On-Demand Single Photons with High Extraction Efficiency and Near-Unity Indistinguishability from a Resonantly Driven Quantum Dot in a Micropillar, Phys. Rev. Lett. **116**, 020401 (2016).

[8] I. Aharonovich, D. Englund, and M. Toth, Solid-state single-photon emitters, Nat. Photonics **10**, 631 (2016).

[9] P. Senellart, G. Solomon, and A. White, High-performance semiconductor quantum-dot single-photon sources, Nat. Nanotechnol. **12**, 1026 (2017).

[10] C. Chakraborty, N. Vamivakas, and D. Englund, Advances in quantum light emission from 2D materials, Nanophotonics **8**, 2017 (2019).

[11] S. Rodt, S. Reitzenstein, and T. Heindel, Deterministically fabricated solid-state quantum-light sources, J. Phys.: Condens. Matter **32**, 153003 (2020).

[12] L. Zhai, G. N. Nguyen, C. Spinnler, J. Ritzmann, M. C. Löbl, A. D. Wieck, A. Ludwig, A. Javadi, and R. J. Warburton, Quantum interference of identical photons from remote GaAs quantum dots, Nat. Nanotechnol. **17**, 829 (2022).

[13] T. Schröder, F. Gädeke, M. J. Banholzer, and O. Benson, Ultrabright and efficient single-photon generation based on nitrogen-vacancy centres in nanodiamonds on a solid immersion lens, New J. Phys. **13**, 055017 (2011).

[14] T. Schröder, S. L. Mouradian, J. Zheng, M. E. Trusheim, M. Walsh, E. H. Chen, L. Li, I. Bayn, and D. Englund, Quantum nanophotonics in diamond, J. Opt. Soc. Am. B **33**, B65 (2016).

[15] M. Leifgen, T. Schröder, F. Gädeke, R. Riemann, V. Métillon, E. Neu, C. Hepp, C. Arend, C. Becher, K. Lauritsen, and O. Benson, Evaluation of nitrogen- and silicon-vacancy defect centres as single photon sources in quantum key distribution, New J. Phys. **16**, 023021 (2014).

[16] D. Englund, B. Shields, K. Rivoire, F. Hatami, J. Vučković, H. Park, and M. D. Lukin, Deterministic coupling of a single nitrogen vacancy center to a photonic crystal cavity, Nano Lett. **10**, 3922 (2010).

[17] K. Beha, H. Fedder, M. Wolfer, M. C. Becker, P. Siyushev, M. Jamali, A. Batalov, C. Hinz, J. Hees, L. Kirste *et al.*, Diamond nanophotonics, Beilstein J. Nanotechnol. **3**, 895 (2012).

[18] K. G. Fehler, A. P. Ovvyan, N. Gruhler, W. H. P. Pernice, and A. Kubanek, Efficient coupling of an ensemble of nitrogen vacancy center to the mode of a high-Q, Si_3N_4 photonic crystal cavity, ACS Nano **13**, 6891 (2019).

[19] E. Janitz, M. K. Bhaskar, and L. Childress, Cavity quantum electrodynamics with color centers in diamond, Optica **7**, 1232 (2020).

[20] P. P. J. Schrinner, J. Olthaus, D. E. Reiter, and C. Schuck, Integration of diamond-based quantum emitters with nanophotonic circuits, Nano Lett. **20**, 8170 (2020).

[21] N. V. Proscia, H. Jayakumar, X. Ge, G. Lopez-Morales, Z. Shotan, W. Zhou, C. A. Meriles, and V. M. Menon, Microcavity-coupled emitters in hexagonal boron nitride, Nanophotonics **9**, 2937 (2020).

[22] J. E. Fröch, S. Kim, N. Mendelson, M. Kianinia, M. Toth, and I. Aharonovich, Coupling hexagonal boron nitride quantum emitters to photonic crystal cavities, ACS Nano **14**, 7085 (2020).

[23] G. Grosso, H. Moon, B. Lienhard, S. Ali, D. K. Efetov, M. M. Furchi, P. Jarillo-Herrero, M. J. Ford, I. Aharonovich, and D. Englund, Tunable and high-purity room temperature single-photon emission from atomic defects in hexagonal boron nitride, Nat. Commun. **8**, 705 (2017).

[24] D. A. Vajner, L. Rickert, T. Gao, K. Kaymazlar, and T. Heindel, Quantum communication using semiconductor quantum dots, Adv. Quantum Technol. **5**, 2100116 (2022).

[25] C. Schimpf, M. Reindl, D. Huber, B. Lehner, S. F. C. D. Silva, S. Manna, M. Vyvlecka, P. Walther, and A. Rastelli, Quantum cryptography with highly entangled photons from semiconductor quantum dots, Sci. Adv. **7**, eabe8905 (2021).

[26] F. B. Basset, M. Valeri, E. Roccia, V. Muredda, D. Poderini, J. Neuwirth, N. Spagnolo, M. B. Rota, G. Carvacho, F. Sciarrino, and R. Trotta, Quantum key distribution with entangled photons generated on demand by a quantum dot, Sci. Adv. **7**, eabe6379 (2021).

[27] M. Müller, S. Bounouar, K. D. Jöns, M. Glässl, and P. Michler, On-demand generation of indistinguishable polarization-entangled photon pairs, Nat. Photonics **8**, 224 (2014).

[28] N. Akopian, N. H. Lindner, E. Poem, Y. Berlatzky, J. Avron, D. Gershoni, B. D. Gerardot, and P. M. Petroff, Entangled Photon Pairs from Semiconductor Quantum Dots, Phys. Rev. Lett. **96**, 130501 (2006).

[29] J. Yin, Y. Cao, Y.-H. Li, S.-K. Liao, L. Zhang, J.-G. Ren, W.-Q. Cai, W.-Y. Liu, B. Li, H. Dai *et al.*, Satellite-based entanglement distribution over 1200 kilometers, Science **356**, 1140 (2017).

[30] D. Huber, M. Reindl, J. Aberl, A. Rastelli, and R. Trotta, Semiconductor quantum dots as an ideal source of polarization-entangled photon pairs on-demand: A review, J. Opt. **20**, 073002 (2018).

[31] J.-W. Pan, Z.-B. Chen, C.-Y. Lu, H. Weinfurter, A. Zeilinger, and M. Żukowski, Multiphoton entanglement and interferometry, Rev. Mod. Phys. **84**, 777 (2012).

[32] R. M. Stevenson, R. J. Young, P. Atkinson, K. Cooper, D. A. Ritchie, and A. J. Shields, A semiconductor source of triggered entangled photon pairs, Nature (London) **439**, 179 (2006).

[33] R. J. Young, R. M. Stevenson, P. Atkinson, K. Cooper, D. A. Ritchie, and A. J. Shields, Improved fidelity of triggered entangled photons from single quantum dots, New J. Phys. **8**, 29 (2006).

[34] R. Hafenbrak, S. M. Ulrich, P. Michler, L. Wang, A. Rastelli, and O. G. Schmidt, Triggered polarization-entangled photon pairs from a single quantum dot up to 30 K, New J. Phys. **9**, 315 (2007).

[35] A. Muller, W. Fang, J. Lawall, and G. S. Solomon, Creating Polarization-Entangled Photon Pairs from a Semiconductor Quantum Dot Using the Optical Stark Effect, Phys. Rev. Lett. **103**, 217402 (2009).

[36] A. Dousse, J. Suffczyński, A. Beveratos, O. Krebs, A. Lemaître, I. Sagnes, J. Bloch, P. Voisin, and P. Senellart, Ultrabright source of entangled photon pairs, Nature (London) **466**, 217 (2010).

[37] R. M. Stevenson, C. L. Salter, J. Nilsson, A. J. Bennett, M. B. Ward, I. Farrer, D. A. Ritchie, and A. J. Shields, Indistinguishable Entangled Photons Generated by a Light-Emitting Diode, Phys. Rev. Lett. **108**, 040503 (2012).

[38] R. Trotta, J. S. Wildmann, E. Zallo, O. G. Schmidt, and A. Rastelli, Highly entangled photons from hybrid piezoelectric-semiconductor quantum dot devices, Nano Lett. **14**, 3439 (2014).

[39] R. Winik, D. Cogan, Y. Don, I. Schwartz, L. Gantz, E. R. Schmidgall, N. Livneh, R. Rapaport, E. Buks, and D. Gershoni, On-demand source of maximally entangled photon pairs using the biexciton-exciton radiative cascade, Phys. Rev. B **95**, 235435 (2017).

[40] D. Huber, M. Reindl, Y. Huo, H. Huang, J. S. Wildmann, O. G. Schmidt, A. Rastelli, and R. Trotta, Highly indistinguishable and strongly entangled photons from symmetric GaAs quantum dots, Nat. Commun. **8**, 15506 (2017).

[41] S. Bounouar, C. de la Haye, M. Strauß, P. Schnauber, A. Thoma, M. Gschrey, J.-H. Schulze, A. Strittmatter, S. Rodt, and S. Reitzenstein, Generation of maximally entangled states and coherent control in quantum dot microlenses, Appl. Phys. Lett. **112**, 153107 (2018).

[42] H. Wang, H. Hu, T.-H. Chung, J. Qin, X. Yang, J.-P. Li, R.-Z. Liu, H.-S. Zhong, Y.-M. He, X. Ding, Y.-H. Deng, Q. Dai, Y.-H. Huo, S. Höfling, C.-Y. Lu, and J.-W. Pan, On-Demand Semiconductor Source of Entangled Photons Which Simultaneously Has High Fidelity, Efficiency, and Indistinguishability, Phys. Rev. Lett. **122**, 113602 (2019).

[43] J. Liu, R. Su, Y. Wei, B. Yao, S. F. C. d. Silva, Y. Yu, J. Iles-Smith, K. Srinivasan, A. Rastelli, J. Li, and X. Wang, A solid-state source of strongly entangled photon pairs with high brightness and indistinguishability, Nat. Nanotechnol. **14**, 586 (2019).

[44] A. Fognini, A. Ahmadi, M. Zeeshan, J. T. Fokkens, S. J. Gibson, N. Sherlekar, S. J. Daley, D. Dalacu, P. J. Poole, K. D. Jöns, V. Zwiller, and M. E. Reimer, Dephasing free photon entanglement with a quantum dot, ACS Photonics **6**, 1656 (2019).

[45] C. Hopfmann, W. Nie, N. L. Sharma, C. Weigelt, F. Ding, and O. G. Schmidt, Maximally entangled and gigahertz-clocked on-demand photon pair source, Phys. Rev. B **103**, 075413 (2021).

[46] M. Cygorek, F. Ungar, T. Seidelmann, A. M. Barth, A. Vagov, V. M. Axt, and T. Kuhn, Comparison of different concurrences characterizing photon pairs generated in the biexciton cascade in quantum dots coupled to microcavities, Phys. Rev. B **98**, 045303 (2018).

[47] T. Seidelmann, F. Ungar, M. Cygorek, A. Vagov, A. M. Barth, T. Kuhn, and V. M. Axt, From strong to weak temperature dependence of the two-photon entanglement resulting from the biexciton cascade inside a cavity, Phys. Rev. B **99**, 245301 (2019).

[48] T. Seidelmann, F. Ungar, A. M. Barth, A. Vagov, V. M. Axt, M. Cygorek, and T. Kuhn, Phonon-Induced Enhancement of Photon Entanglement in Quantum Dot-Cavity Systems, Phys. Rev. Lett. **123**, 137401 (2019).

[49] T. H. Stievater, X. Li, D. G. Steel, D. Gammon, D. S. Katzer, D. Park, C. Piermarocchi, and L. J. Sham, Rabi Oscillations of Excitons in Single Quantum Dots, Phys. Rev. Lett. **87**, 133603 (2001).

[50] H. Kamada, H. Gotoh, J. Temmyo, T. Takagahara, and H. Ando, Exciton Rabi Oscillation in a Single Quantum Dot, Phys. Rev. Lett. **87**, 246401 (2001).

[51] A. Ramsay, A review of the coherent optical control of the exciton and spin states of semiconductor quantum dots, Semicond. Sci. Technol. **25**, 103001 (2010).

[52] C.-M. Simon, T. Belhadj, B. Chatel, T. Amand, P. Renucci, A. Lemaitre, O. Krebs, P. A. Dalgarno, R. J. Warburton, X. Marie, and B. Urbaszek, Robust Quantum Dot Exciton Generation via Adiabatic Passage with Frequency-Swept Optical Pulses, Phys. Rev. Lett. **106**, 166801 (2011).

[53] Y. Wu, I. M. Piper, M. Ediger, P. Brereton, E. R. Schmidgall, P. R. Eastham, M. Hugues, M. Hopkinson, and R. T. Phillips, Population Inversion in a Single InGaAs Quantum Dot Using the Method of Adiabatic Rapid Passage, Phys. Rev. Lett. **106**, 067401 (2011).

[54] T. Kaldewey, S. Lüker, A. V. Kuhlmann, S. R. Valentin, J.-M. Chauveau, A. Ludwig, A. D. Wieck, D. E. Reiter, T. Kuhn, and R. J. Warburton, Demonstrating the decoupling regime of the electron-phonon interaction in a quantum dot using chirped optical excitation, Phys. Rev. B **95**, 241306(R) (2017).

[55] R. Mathew, E. Dilcher, A. Gamouras, A. Ramachandran, H. Y. S. Yang, S. Freisem, D. Deppe, and K. C. Hall, Subpicosecond adiabatic rapid passage on a single semiconductor quantum dot: Phonon-mediated dephasing in the strong-driving regime, Phys. Rev. B **90**, 035316 (2014).

[56] A. Debnath, C. Meier, B. Chatel, and T. Amand, Chirped laser excitation of quantum dot excitons coupled to a phonon bath, Phys. Rev. B **86**, 161304(R) (2012).

[57] C. Matthiesen, A. N. Vamivakas, and M. Atatüre, Subnatural Linewidth Single Photons from a Quantum Dot, Phys. Rev. Lett. **108**, 093602 (2012).

[58] A. V. Kuhlmann, J. Houel, D. Brunner, A. Ludwig, D. Reuter, A. D. Wieck, and R. J. Warburton, A dark-field microscope for background-free detection of resonance fluorescence from single semiconductor quantum dots operating in a set-and-forget mode, Rev. Sci. Instrum. **84**, 073905 (2013).

[59] P.-L. Ardelt, L. Hanschke, K. A. Fischer, K. Müller, A. Kleinkauf, M. Koller, A. Bechtold, T. Simmet, J. Wierzbowski, H. Riedl, G. Abstreiter, and J. J. Finley, Dissipative preparation of the exciton and biexciton in self-assembled quantum dots on picosecond time scales, Phys. Rev. B **90**, 241404(R) (2014).

[60] S. Bounouar, M. Müller, A. M. Barth, M. Glässl, V. M. Axt, and P. Michler, Phonon-assisted robust and deterministic two-photon biexciton preparation in a quantum dot, Phys. Rev. B **91**, 161302(R) (2015).

[61] J. H. Quilter, A. J. Brash, F. Liu, M. Glässl, A. M. Barth, V. M. Axt, A. J. Ramsay, M. S. Skolnick, and A. M. Fox, Phonon-Assisted Population Inversion of a Single InGaAs/GaAs Quantum Dot by Pulsed Laser Excitation, Phys. Rev. Lett. **114**, 137401 (2015).

[62] A. M. Barth, S. Lüker, A. Vagov, D. E. Reiter, T. Kuhn, and V. M. Axt, Fast and selective phonon-assisted state preparation

of a quantum dot by adiabatic undressing, Phys. Rev. B **94**, 045306 (2016).

[63] G. R. Wilbur, A. Binai-Motlagh, A. Clarke, A. Ramachandran, N. Milson, J. P. Healey, S. O'Neal, D. G. Deppe, and K. C. Hall, Notch-filtered adiabatic rapid passage for optically driven quantum light sources, APL Photonics **7**, 111302 (2022).

[64] F. Sbresny, L. Hanschke, E. Schöll, W. Rauhaus, B. Scaparra, K. Boos, E. Zubizarreta Casalengua, H. Riedl, E. del Valle, J. J. Finley, K. D. Jöns, and K. Müller, Stimulated Generation of Indistinguishable Single Photons from a Quantum Ladder System, Phys. Rev. Lett. **128**, 093603 (2022).

[65] R. Uppu, F. T. Pedersen, Y. Wang, C. T. Olesen, C. Papon, X. Zhou, L. Midolo, S. Scholz, A. D. Wieck, A. Ludwig, and P. Lodahl, Scalable integrated single-photon source, Sci. Adv. **6**, eabc8268 (2020).

[66] H. Wang, Y.-M. He, T. H. Chung, H. Hu, Y. Yu, S. Chen, X. Ding, M. C. Chen, J. Qin, X. Yang, R.-Z. Liu, Z. C. Duan, J. P. Li, S. Gerhardt, K. Winkler, J. Jurkat, L.-J. Wang, N. Gregersen, Y.-H. Huo, Q. Dai, *et al.*, Towards optimal single-photon sources from polarized microcavities, Nat. Photonics **13**, 770 (2019).

[67] N. Tomm, A. Javadi, N. O. Antoniadis, D. Najer, M. C. Löbl, A. R. Korsch, R. Schott, S. R. Valentin, A. D. Wieck, A. Ludwig, and R. J. Warburton, A bright and fast source of coherent single photons, Nat. Nanotechnol. **16**, 399 (2021).

[68] X. Zhou, P. Lodahl, and L. Midolo, In-plane resonant excitation of quantum dots in a dual-mode photonic-crystal waveguide with high β-factor, Quantum Sci. Technol. **7**, 025023 (2022).

[69] T. K. Bracht, M. Cosacchi, T. Seidelmann, M. Cygorek, A. Vagov, V. M. Axt, T. Heindel, and D. E. Reiter, Swing-up of quantum emitter population using detuned pulses, PRX Quantum **2**, 040354 (2021).

[70] Z.-C. Shi, Y.-H. Chen, W. Qin, Y. Xia, X. X. Yi, S.-B. Zheng, and F. Nori, Two-level systems with periodic n-step driving fields: Exact dynamics and quantum state manipulations, Phys. Rev. A **104**, 053101 (2021).

[71] T. K. Bracht, T. Seidelmann, T. Kuhn, V. M. Axt, and D. E. Reiter, Phonon wave packet emission during state preparation of a semiconductor quantum dot using different schemes, Phys. Status Solidi B **259**, 2100649 (2022).

[72] Y. Karli, F. Kappe, V. Remesh, T. K. Bracht, J. Münzberg, S. Covre da Silva, T. Seidelmann, V. M. Axt, A. Rastelli, D. E. Reiter, and G. Weihs, Super scheme in action: Experimental demonstration of red-detuned excitation of a quantum emitter, Nano Lett. **22**, 6567 (2022).

[73] K. Boos, F. Sbresny, S. K. Kim, M. Kremser, H. Riedl, F. W. Bopp, W. Rauhaus, B. Scaparra, K. D. Jöns, J. J. Finley, K. Müller, and L. Hanschke, Coherent dynamics of the swing-up excitation technique, arXiv:2211.14289.

[74] Y.-M. He, H. Wang, C. Wang, M.-C. Chen, X. Ding, J. Qin, Z.-C. Duan, S. Chen, J.-P. Li, R.-Z. Liu *et al.*, Coherently driving a single quantum two-level system with dichromatic laser pulses, Nat. Phys. **15**, 941 (2019).

[75] Z. X. Koong, E. Scerri, M. Rambach, M. Cygorek, M. Brotons-Gisbert, R. Picard, Y. Ma, S. I. Park, J. D. Song, E. M. Gauger, and B. D. Gerardot, Coherent Dynamics in Quantum Emitters under Dichromatic Excitation, Phys. Rev. Lett. **126**, 047403 (2021).

[76] L. Vannucci and N. Gregersen, Phonon-decoupled di-chromatic pumping scheme for highly efficient and indistinguishable single-photon sources, arXiv:2209.07770.

[77] S. Lüker, K. Gawarecki, D. E. Reiter, A. Grodecka-Grad, V. M. Axt, P. Machnikowski, and T. Kuhn, Influence of acoustic phonons on the optical control of quantum dots driven by adiabatic rapid passage, Phys. Rev. B **85**, 121302(R) (2012).

[78] S. Lüker, T. Kuhn, and D. E. Reiter, Phonon-assisted dark exciton preparation in a quantum dot, Phys. Rev. B **95**, 195305 (2017).

[79] D. Tannor, *Introduction to Quantum Mechanics* (University Science Books, Sausalito, CA, 2007).

[80] S. Lüker and D. E. Reiter, A review on optical excitation of semiconductor quantum dots under the influence of phonons, Semicond. Sci. Technol. **34**, 063002 (2019).

[81] D. E. Reiter, T. Kuhn, and V. M. Axt, Distinctive characteristics of carrier-phonon interactions in optically driven semiconductor quantum dots, Adv. Phys.: X **4**, 1655478 (2019).

[82] M. Neumann, F. Kappe, T. K. Bracht, M. Cosacchi, T. Seidelmann, V. M. Axt, G. Weihs, and D. E. Reiter, Optical stark shift to control the dark exciton occupation of a quantum dot in a tilted magnetic field, Phys. Rev. B **104**, 075428 (2021).

[83] L. Schweickert, K. D. Jöns, K. D. Zeuner, S. F. Covre da Silva, H. Huang, T. Lettner, M. Reindl, J. Zichi, R. Trotta, A. Rastelli, and V. Zwiller, On-demand generation of background-free single photons from a solid-state source, Appl. Phys. Lett. **112**, 093106 (2018).

[84] T. Seidelmann, C. Schimpf, T. K. Bracht, M. Cosacchi, A. Vagov, A. Rastelli, D. E. Reiter, and V. M. Axt, Two-Photon Excitation Sets Limit to Entangled Photon Pair Generation from Quantum Emitters, Phys. Rev. Lett. **129**, 193604 (2022).